Modulation of excitation–contraction coupling by isoproterenol in cardiomyocytes with controlled SR Ca^{2+} load and Ca^{2+} current trigger

Kenneth S. Ginsburg and Donald M. Bers

Department of Physiology, Loyola University Chicago, Stritch School of Medicine, Maywood, IL 60153, USA

Cardiac Ca^{2+} transients are enhanced by cAMP-dependent protein kinase (PKA). However, PKA-dependent modulation of ryanodine receptor (RyR) function in intact cells is difficult to measure, because PKA simultaneously increases Ca^{2+} current (I_{Ca}), SR Ca^{2+} uptake and SR Ca^{2+} loading (which independently increase SR Ca^{2+} release). We measured I_{Ca} and SR Ca^{2+} release $\pm$ 1 μm isoproterenol (ISO; isoprenaline) in voltage-clamped ventricular myocytes of rabbits and transgenic mice (expressing only non-phosphorylatable phospholamban). This mouse model helps control for any effect of ISO-enhanced SR uptake on observed release, but the two species produced essentially identical results. SR Ca^{2+} load and I_{Ca} were adjusted by conditioning. We thus evaluated PKA effects on SR Ca^{2+} release at constant SR Ca^{2+} load and I_{Ca} trigger (with constant unitary I_{Ca}). The amount of SR Ca^{2+} release increased as a function of either I_{Ca} or SR Ca^{2+} load, but ISO did not alter the relationships (measured as gain or fractional release). This was true over a wide range of SR Ca^{2+} load and I_{Ca}. However, the maximal rate of SR Ca^{2+} release was $\sim$50% faster with ISO (at most loads and I_{Ca} levels). We conclude that the isolated effect of PKA on SR Ca^{2+} release is an increase in maximal rate of release and faster turn-off of release (such that integrated SR Ca^{2+} release is unchanged). The increased amount of SR Ca^{2+} release normally seen with ISO depends primarily on increased I_{Ca} trigger and SR Ca^{2+} load, whereas faster release kinetics may be the main result of RyR phosphorylation.

(Received 18 September 2003; accepted after revision 9 January 2004; first published online 14 January 2004)
Corresponding author D. M. Bers: Department of Physiology, Loyola University Chicago, Stritch School of Medicine, Maywood, IL 60153, USA. Email: dbers@lumc.edu

Cardiac manifestations of adrenergic stimulation (inotropy, chronotropy and lusitropy) were already under investigation by 1900 (Elliott, 1905). Via protein kinase A (PKA) activation, β-adrenergic receptor (β-AR) activation promotes phosphorylation of at least four cellular targets which have key roles in the control of excitation–contraction coupling (ECC) and Ca^{2+}-induced Ca^{2+} release (CICR). PKA-dependent phosphorylation of: (1) troponin-I (TnI) reduces myofilament Ca^{2+} sensitivity (Zhang *et al.* 1995), (2) L-type Ca^{2+} channels increases Ca^{2+} current (I_{Ca}, due mainly to increased open probability; Bean *et al.* 1984), (3) phospholamban (PLB) enhances SR Ca^{2+}-ATPase activity and SR Ca^{2+} load (by disinhibiting SR Ca^{2+}-ATPase; Lindemann *et al.* 1983), (4) ryanodine receptor/Ca^{2+} release channels (RyR) can alter function as described below (Yoshida *et al.* 1992; Marx *et al.* 2000). Since non-subtype-selective β-AR agonists like isoproterenol (ISO) normally phosphorylate all these targets simultaneously, the balance of effects on ECC in the intact cell is complex. This study evaluates how PKA-dependent RyR phosphorylation affects RyR behaviour during ECC, independently of effects on I_{Ca}, TnI or PLB.

In cardiac RyRs in isolation in lipid bilayers (in steady state), PKA activation led to enhanced open probability (P_o) and appearance of submaximal conductance states, with a net increase in integrated Ca^{2+} flux (Marx *et al.* 2000, 2001). These PKA effects were correlated with unbinding of the FK-506 binding protein (FKBP-12.6) from the RyR, where FKBP-12.6 bound to RyR normally stabilizes and coordinates RyR gating, minimizing substate occurrence and SR Ca^{2+} leak (Marx *et al.* 2001; Prestle *et al.* 2001). On the other hand, Valdivia *et al.* (1995) showed that PKA decreased steady-state RyR P_o in bilayers, but enhanced the transient peak P_o in response to a rapid rise in activating [Ca^{2+}] (meant to simulate what happens in

 DOI: 10.1113.jphysiol.2003.055384

ECC). Extrapolating these disparate RyR bilayer results to intact cells, we might or might not expect enhanced SR Ca^{2+} release with PKA (for a given I_{Ca} trigger and SR Ca^{2+} load).

Li *et al.* (2002) studied PKA effects on resting Ca^{2+} sparks in intact and permeabilized ventricular myocytes, thereby retaining RyR in a more physiological local environment. Ca^{2+} sparks reflect the stochastic resting openings of clusters of RyRs and are probably the main route of Ca^{2+} leak from the SR (Cheng *et al.* 1993; Bers, 2001). PKA greatly stimulated Ca^{2+} spark frequency in these myocytes, but only when PLB could be phosphorylated (which caused SR Ca^{2+} load to increase). In mice that either lack PLB or express only a mutant PLB which lacks both the Ser^{16} and Thr^{17} regulatory phosphorylation sites (the latter used also in the present study), Ca^{2+} spark frequency and characteristics were unchanged, despite direct evidence of RyR phosphorylation. Evidently, PKA activation does not affect RyR leak much during rest. However, the situation could be quite different during ECC where I_{Ca} triggers RyR opening. Intact stimulated cells are required to assess this.

With β-AR stimulation, larger and faster relaxing $[Ca^{2+}]_i$ transients are routinely observed in cardiac myocytes (Callewaert *et al.* 1988), and the typical bell-shaped dependence of $[Ca^{2+}]_i$ transients on membrane voltage usually becomes flat-topped (Hussain & Orchard, 1997). However, in these studies, both the I_{Ca} trigger and SR Ca^{2+} load increased simultaneously with ISO. Since both load and trigger strongly affect ECC/CICR independently of β-AR modulation (Bassani *et al.* 1995*b*; Shannon *et al.* 2000), these studies do not reveal how intrinsic RyR function is altered independently of I_{Ca} or SR Ca^{2+} load changes.

β-AR stimulation led to more spatially organized and time-synchronized depolarization-induced Ca^{2+} release in rat ventricular myocytes (Song *et al.* 2001) and post-infarct border zone rabbit myocytes (Litwin *et al.* 1998). The former reported a decrease of ECC gain with ISO, but in that study most I_{Ca} triggers with ISO were large, a possibly saturating condition where we see ECC gain to be at its lowest with or without ISO (note that ECC gain is usually some function of Ca^{2+} release/I_{Ca}). In contrast, Viatchenko-Karpinski & Györke (2001) found increased ECC gain with ISO, but only when both intra- and extracellular Na^+ were present (implying a role of Na^+–Ca^{2+} exchange, which can alter the spatial properties and stability of the Ca^{2+} trigger; Sham, 2000). delPrincipe *et al.* (2001) also detected an ISO-mediated increase in ECC gain, especially near threshold. They used a controlled flash-photolytic Ca^{2+} trigger (rather than I_{Ca}), in cells at constant SR load. While this technique offers close control of the Ca^{2+} trigger, it is less physiological than I_{Ca}. Taken together, these disparate results indicate that Ca^{2+} release in active cells is strongly dependent on specifics of the trigger and SR Ca^{2+} load.

A unique feature of our experiments is that we compared fractional SR Ca^{2+} release (and ECC gain) ± ISO over a broad range of controlled I_{Ca} triggers and SR Ca^{2+} loads. We used steady-state pre-inactivation of I_{Ca} to control I_{Ca} (rather than test membrane potential (E_m) or external $[Ca^{2+}]$). This helped us adjust triggers with ISO over a wide range, including moderate non-saturating values expected during APs. In fact ISO *versus* control comparisons were made at comparable macroscopic I_{Ca} and identical unitary I_{Ca} amplitude, test voltage and external $[Ca^{2+}]$. We used varying conditioning pulses to obtain overlapping SR Ca^{2+} loads (± ISO). This extends our previous strategy (Li *et al.* 1997) where we showed that calmodulin-dependent protein kinase II (CaMKII) activation profoundly enhanced SR Ca^{2+} release for a given I_{Ca} and SR Ca^{2+} load (over a range of I_{Ca} triggers).

Further, although we used mainly rabbit ventricular myocytes, we also used a recently developed mouse model expressing only mutant PLB where both phosphorylation sites (Ser^{16} and Thr^{17}) are mutated to Ala. This mutant PLB was reintroduced in the PLB knockout (Luo *et al.* 1994) background. The SR Ca^{2+}-ATPase in this model has a Ca^{2+} affinity comparable to wild-type mice, but cannot be stimulated by ISO (Brittsan *et al.* 2003). This made it both easier to control SR Ca^{2+} loading ± ISO, and also prevented the acceleration of $[Ca^{2+}]_i$ decline seen in ISO (which could complicate Ca^{2+} release analysis).

Here we find, as expected, that under fixed conditions (either control or ISO), increasing I_{Ca} or SR Ca^{2+} load enhance fractional SR Ca^{2+} release (and enhanced SR Ca^{2+} load enhances ECC gain). For comparable I_{Ca} and SR Ca^{2+} load, ISO had little effect on either SR fractional release or ECC gain, but did cause a significant increase in the SR Ca^{2+} release rate.

Methods

Cell preparation

All cells were isolated using species-specific protocols approved by Loyola University's Institutional Animal Care and Use Committee (IACUC). The nominally Ca^{2+}-free cell isolation solution was either Tyrode solution (mM: NaCl 140, KCl 4, $MgCl_2$ 1, and Hepes 10; pH 7.2) or Dulbecco's minimal essential medium gassed with 95% O_2–5% CO_2 (DMEM; Type 22300, Gibco/Invitrogen,

USA). Rabbits were anaesthetized with sodium pentobarbital (50 mg kg^{-1} I.V.) and deep anaesthesia verified (complete absence of reflex on repeated corneal touch and foot pinch). Hearts were excised (at which time the animal died of exsanguination), rinsed in ice-cold Ca^{2+}-free solution, and retrogradely perfused at 37°C, at either constant flow (30–36 ml min^{-1}) or preferably constant pressure (80 mmHg). After 5 min of perfusion with Ca^{2+}-free solution, collagenase (0.3–0.7 mg ml^{-1}; Yakult Corporation, Japan or Boehringer Mannheim, Germany) and Ca^{2+} (10–20 μM) were added. After 15–25 min, perfusion was stopped and ventricles were minced into ~2 mm^3 size pieces. Optionally the pieces were incubated for 5–20 min in fresh enzyme. Finally, enzyme activity was stopped with DMEM solution containing bovine serum albumin (BSA; 0.5–1%), and tissue was agitated or triturated to liberate single cells. These were washed and stored in DMEM solution adjusted to $[Ca^{2+}] = 150$ μM.

Mice were anaesthetized (inhalation of 2–3% isoflurane in 100% O_2), tracheotomized and mechanically ventilated. Upon verifying total insentience (complete absence of reflex on repeated corneal touch and foot pinch), we opened the chest cavity, injected cold high-K^+ cardioplegia solution into the vena cava, quickly excised the heart (at which time the mouse died of exsanguination), and transferred it to our gravity-driven (80 mmHg) apparatus for perfusion at 37°C. The initial flow rate, ~3 ml min^{-1}, increased during digestion, and this increase was a criterion for ending perfusion. After enzyme perfusion the mouse hearts were further treated as described above for rabbit. All mice were the PLB double mutants described in the introduction.

Fluorescent measurement of $[Ca^{2+}]_i$

Cells were plated on single-use laminin-coated glass cover slips and mounted on an epifluorescence microscope. We loaded rabbit cells with 10 μM indo-1 AM, applied externally for 22–27 min at 23°C, and allowed an equal time for washing and de-esterification. Indo-1 was excited at 365 ± 5 nm and emitted fluorescence (405 ± 10 nm and 485 ± 10 nm) was recorded at 100 Hz bandwidth. The background-subtracted ratio (R) of fluorescence at 405 nm *versus* 485 nm was converted to $[Ca^{2+}]_i$ using $[Ca^{2+}]_i = K_d\beta(R - R_{min})/(R_{max} - R)$ (Grynkiewicz *et al.* 1985). R_{min}, R_{max}, and β were determined and K_d was taken as 844 nm (Bassani *et al.* 1995*a*).

Mouse (and some rabbit) myocytes were loaded with fluo-3 AM for 25–40 min, with a comparable de-esterification time. Cells were excited at 480 ± 5 nm, and emission was recorded at 535 ± 20 nm $[Ca^{2+}]_i$, was determined using (Cheng *et al.* 1993):

$$[Ca^{2+}]_i = K_{dR}/((K_d/[Ca^{2+}]_{rest}) + 1 - R),$$

where R was emitted fluorescence divided by resting emitted fluorescence, each after background subtraction. $[Ca^{2+}]_{rest}$ was taken as 100 nM, and $K_d = 1100$ nM was used to calculate $[Ca^{2+}]_i$. No difference in results was evident between the two indicators.

Solutions and recording conditions

I_{Ca} was recorded in perforated patch whole cell voltage clamp (120 μg ml^{-1} amphotericin-B) to prevent rundown. Capacitance was cancelled and series resistance was compensated as needed. Cells were recorded in a modified Tyrode solution containing (mM: NaCl 140, CsCl 4, $MgCl_2$ 1, $CaCl_2$ 1 (for mouse) or 2 (for rabbit), and Hepes 10; pH 7.4 at 23°C) with niflumate (30 μM) included to block Cl^- currents. ISO was freshly made (<1.5 h before use) and added at 0.3–1 μM. This same solution with caffeine (10 mM) added was rapidly applied for SR Ca^{2+} load measurements. The pipette solution contained 40 mM CsCl and 80 mM of either caesium methanesulphonate or caesium glutamate, Hepes 10 mM (pH 7.2), 1 mM $MgCl_2$ and 1 mMKCl, the latter to ensure a counter-ion supply for SR Ca^{2+} release (Litwin *et al.* 1998). The liquid junction potential (13 mV, pipette negative) was corrected. We kept the pipette solution Na^+ free and I_{Na} inactivated (see below) to minimize subsarcolemmal $[Na^+]$ and avoid Ca^{2+} influx via outward Na^+–Ca^{2+} exchange current (I_{NaCaX}). These solutions assured that all depolarization-activated current was I_{Ca} and that all Na^+–Ca^{2+} exchange current flowed as post-pulse inward tail current (Trafford *et al.* 1997).

Measurement of SR Ca^{2+} load

SR Ca^{2+} content was measured relative to non-mitochondrial cell volume as described (Ginsburg *et al.* 1998). $[Ca^{2+}]_i$ at rest and at peak during caffeine application were each converted to total cytosolic Ca^{2+} considering Ca^{2+} binding at high and low affinity sites and by the fluorophore ($[Ca]_T = [Ca^{2+}]_i + 203\ \mu M/(1 + 420\ nM/[Ca^{2+}]_i) + 703\ \mu M/(1 + 79000\ nM/[Ca^{2+}]_i) + 50\ \mu M/(1 + 1000\ nM/[Ca^{2+}]_i$; Hove-Madsen & Bers, 1993; Bers, 2001), and the difference ($\Delta[Ca]_T$) was taken as the SR Ca^{2+} load. In most cells, caffeine-induced I_{NaCaX} was recorded and fitted, and the fit was integrated (Varro *et al.* 1993), for an additional confirmatory measure of SR Ca^{2+} content.

Recording protocols

Figure 1*A* shows the protocol used in all experiments except those in Fig. 2 to condition the SR to a particular load and then evoke twitch responses. SR loading was adjusted by changing the number of pulses ($n = 15$) at 0.25 Hz, their depolarization level and/or duration as needed. After a conditioning series, one of usually six different test trigger amplitudes was applied. The trigger strength was adjusted by pre-inactivation of I_{Ca} at various holding potentials (V_{hold}) levels for 4 s after the conditioning, but all test triggers were depolarizations to 0 mV. As shown by example in Fig. 1*C* (with both sets of I_{Ca} from the same cell), trigger strength could be adjusted over a similar range ± ISO (grey background), by shifting the range of pre-inactivating E_m. Cells were held at −90 mV between trials to promote inward I_{NaCaX} and thereby minimize SR reloading independently of the applied conditioning, but in order to keep I_{Na} inactivated, V_{hold} was never negative of −55 mV during a trial. As shown in Fig. 1*B*, after the six sequences of conditioning–test twitch we applied a final identical conditioning series followed by caffeine (10 mM) to measure the corresponding SR load.

Data treatment

Peak $[Ca^{2+}]_i$ and time to peak were found directly from the traces for both twitch- and caffeine-induced transients. We determined other features of $[Ca^{2+}]_i$ by fitting, which overcomes subjectivity and variation due to noise. The decaying portions of all $[Ca^{2+}]_i$ transients in a given series (sharing one SR load) were fitted to establish the decay time constant τ, with all sharing a common asymptote for that series. This fitted asymptote was taken as the baseline, to make maximum use of the data and avoid bias in case $[Ca^{2+}]_i$ did not decay quite fully within a record. Twitch amplitude was the difference between peak and asymptotic values. After all decays were fitted, rising phases of twitch $[Ca^{2+}]_i$ were fitted to a Boltzmann sigmoidal function:

$$[Ca^{2+}]_i = \text{base} + (\text{peak} - \text{base})/(1 + \exp((t_{1/2} - t)/\text{slope})),$$

to establish the maximum rate of rise and its time of occurrence.

Peak I_{Ca} and time to peak were found directly from the traces. To establish ΔI_{Ca} and a baseline for integration, I_{Ca} decay post peak was fitted to a weighted sum of two exponentials with asymptote. Only the depolarized region of I_{Ca} (always at 0 mV) was fitted, so no leak correction was needed. All I_{Ca} values in a given series (sharing one SR load) were readily fitted with a common asymptote (prediction for 0 mV at $t = \infty$). Using the long decaying portion of I_{Ca} to determine a common baseline minimized uncertainty, especially for smaller I_{Ca} which may be critical in assessing ECC gain changes. Recorded current often shifted outward with ISO (presumably due to unsuppressed CFTR Cl^- channel current), but by defining I_{Ca} as peak minus fitted

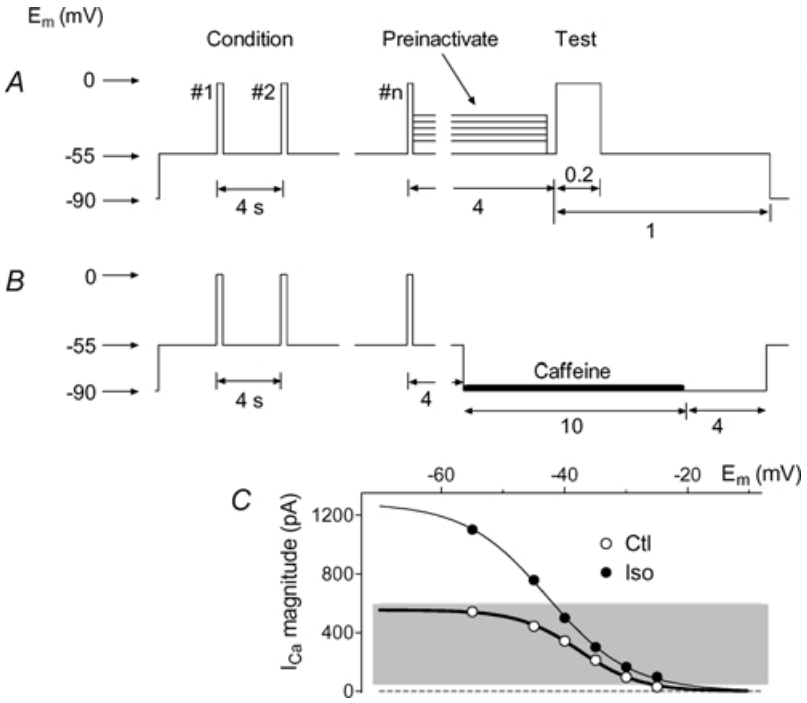

Figure 1. Experimental protocol
A, voltage clamp protocol to evoke twitch contractions with various sized I_{Ca} in a cell whose SR was repeatedly loaded with the same conditioning regime. Pre-inactivation followed by depolarization, always to 0 mV, was used to vary I_{Ca} without changing unitary Ca^{2+} flux. *B*, immediately after the protocol shown in *A*, the same conditioning was repeated, followed by application of 10 mM caffeine, to measure the conditioned load. *C*, example showing substantially overlapping (grey background) I_{Ca} magnitudes attained ± ISO by adjusting pre-inactivation voltage (all traces from same cell).

baseline (all at 0 mV) we removed any influence of this shift. All I_{Ca} in Figs 2–5 were adjusted for plotting so that the fitted asymptote fell on the dotted line. Error bars in figures are ± S.E.M.

Results

We obtained 105 sets of (normally 6) trigger I_{Ca}–SR release $\Delta[Ca^{2+}]_i$ couples with a corresponding SR load from 37 cells (28 rabbit, 9 mouse). This resulted in 664 individual trigger–release couples. We combined rabbit and mouse data, because there were no discernible differences (except where specifically noted below; Fig. 12*B*) when they were analysed separately.

Canonical ISO effects

Figure 2 shows that both I_{Ca} and the $[Ca^{2+}]_i$ transient from a rabbit (*A*) and a mouse (*B*) cell increased on ISO addition (blue traces). In these records we did not specifically control trigger or SR Ca^{2+} loading. Instead of using the protocol in Fig. 1, we depolarized cells infrequently ($\leq$ 0.05 Hz) to promote maximal I_{Ca} availability. In rabbit, but not mouse (lacking phosphorylatable PLB), the $[Ca^{2+}]_i$ transient decayed faster with ISO (note crossover of traces in rabbit). Uncontrolled I_{Ca}–$[Ca^{2+}]_i$ pairs were obtained from most cells with paired control–ISO data (including washout, not shown, in some cases), to confirm that ISO produced its expected effects in our situation, and also that the cells did not run down. *C* and *D* in Fig. 2 show, respectively, that both I_{Ca} and $[Ca^{2+}]_i$ amplitude increased substantially in rabbit. As expected, the time constant (τ) for monoexponentially fitted $[Ca^{2+}]_i$ decay decreased in rabbit by 53% (from 700 ± 128 to 329 ± 64 ms; $n = 10$ cells; $P < 0.05$, not shown). Similar increases in I_{Ca} and $[Ca^{2+}]_i$ amplitude occurred, but decay τ was less affected, as expected in the PLB mutant mouse (see Fig. 2*B*). An ISO-mediated increase of I_{Ca} and $[Ca^{2+}]_i$ without any change in decay kinetics has been verified previously in this model (Brittsan *et al.* 2003).

Ca^{2+} release with matched triggers and SR loads

Figure 3*A* shows twitch $[Ca^{2+}]_i$ and I_{Ca} recorded ± ISO using the protocol in Fig. 1. Traces were selected where the trigger I_{Ca} and SR Ca^{2+} load (Fig. 3*B*) were very closely matched. An appropriate range of I_{Ca} triggers was obtained by pre-inactivating at −45 mV in ISO *versus* −55 mV in control. In this example, from a DM mouse myocyte, the Ca^{2+} transients ± ISO are virtually identical. There is a minor increase in I_{Ca} decay rate with ISO (a point we will consider below). This would suggest that ISO has only very minor effects on overall RyR behaviour during ECC, but as shown in the inset (Fig. 3*A*, left) the maximal rate of rise of $[Ca^{2+}]_i$ also increased discernibly.

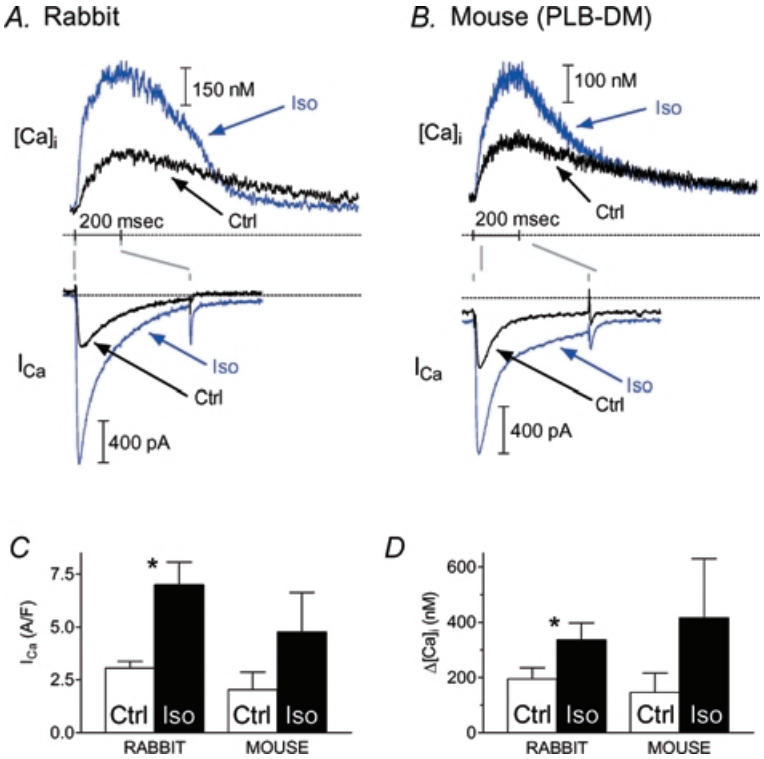

Figure 2. ISO effects with uncontrolled I_{Ca} trigger and SR Ca^{2+} load
In cells stimulated infrequently ($\leq$ 0.05 Hz) to maximize I_{Ca} recovery, but otherwise without specific control of trigger and load, I_{Ca} and $[Ca^{2+}]_i$ increased on adding ISO (blue traces) in both rabbit (*A*) and DM mouse (*B*). $[Ca^{2+}]_i$ transient decay accelerated in rabbit but not in DM mouse. *C* and *D*, average I_{Ca} density and $[Ca^{2+}]_i$ transient size in rabbit ($n = 10$; $^*P \leq 0.05$, Student's *t* test) and mouse ($n = 3$; not tested).

Statistical testing for differences in Ca^{2+} release and ECC gain ± ISO would ideally be based on directly paired records like those in Fig. 3. However, it was difficult to match both trigger and load precisely in a record pair, and as we show next, independently of ISO, Ca^{2+} release depends profoundly on both. Accordingly we developed release/gain functions which describe each record. These functions were then compared over corresponding trigger and load ranges.

Ca^{2+} release was strongly affected by trigger and SR load

Figure 4, shows that, independently of ISO, increasing SR Ca^{2+} load increased twitch Ca^{2+} release when trigger I_{Ca} was held constant. Figure 4*A* shows larger and smaller SR loads, while Fig. 4*B* and *C* shows twitch $[Ca^{2+}]_i$ and I_{Ca} for two different trigger strengths at the respective loads. The rabbit cell in these records was not treated with ISO, but later gave a robust ISO response (not shown). Because the I_{Ca} trigger was constant in both *B* and *C* in Fig. 4, the different transient amplitudes indicate a load-dependent change in ECC gain.

Figure 5 (from another rabbit cell) shows that (independently of ISO) SR Ca^{2+} release increased with increasing I_{Ca} trigger strength. The larger amplitude I_{Ca} series (*A*) graded Ca^{2+} release over a larger range than the smaller I_{Ca} series (*B*), while the SR Ca^{2+} loading was nearly constant (106.9 μmol (l cytosol)$^{-1}$ for the large trigger series *versus* 115.3 for the small series). All traces in this example were recorded with ISO. It is notable that pre-inactivation in the range of −45 to −25 mV produced small graded responses, despite the presence of ISO and despite the slightly higher SR Ca^{2+} loading in the pre-inactivated series (i.e. any sensitization of Ca^{2+} release by ISO should be apparent with these small triggers). For these two twitch series, release as a function of peak I_{Ca} trigger fell along a single saturating function (inset, upper left). Twitches due to fully activated I_{Ca} (not shown) recorded before and after these two series showed that this cell was strongly responsive to ISO and did not run down.

Ca^{2+} release and gain functions at constant SR load

Figure 6 shows how we obtained one Ca^{2+} release and one ECC gain function for free $[Ca^{2+}]$, along with corresponding functions for total $[Ca^{2+}]$, as well as a maximum rate of rise and time to maximum rate of rise (not shown) from each set of six twitches (Fig. 6*A*) with a corresponding SR load (Fig. 6*B*). Figure 6*A* shows curves fitted separately for rise and decay segments of $[Ca^{2+}]_i$ transients and I_{Ca} decay.

Figure 6*B* shows fits for the decay of the caffeine-evoked free $[Ca^{2+}]_i$ transient (top, biexponential) and the entire Na^+–Ca^{2+} exchange current (bottom, sigmoidal rise/exponential decay), used to determine SR Ca^{2+} loads.

To allow a comparison of responses among twitch sets over useful ranges of peak I_{Ca} and Ca^{2+} influx values, we fitted each set of Ca^{2+} release data to a three-parameter saturating function, e.g. sigmoidal, piecewise linear, etc., as shown in Fig. 6*C* (points: data; curve: fit) for free $\Delta[Ca^{2+}]_i$ and Fig. 6*D* for total calcium. Total calcium release was defined as twitch $\Delta[Ca]_T - \int I_{Ca}dt$ (the change in total $[Ca^{2+}]$ due to release with the cumulated Ca^{2+} influx removed), with $\int I_{Ca}dt$ measured with respect to the I_{Ca} common asymptote. Integration was started when

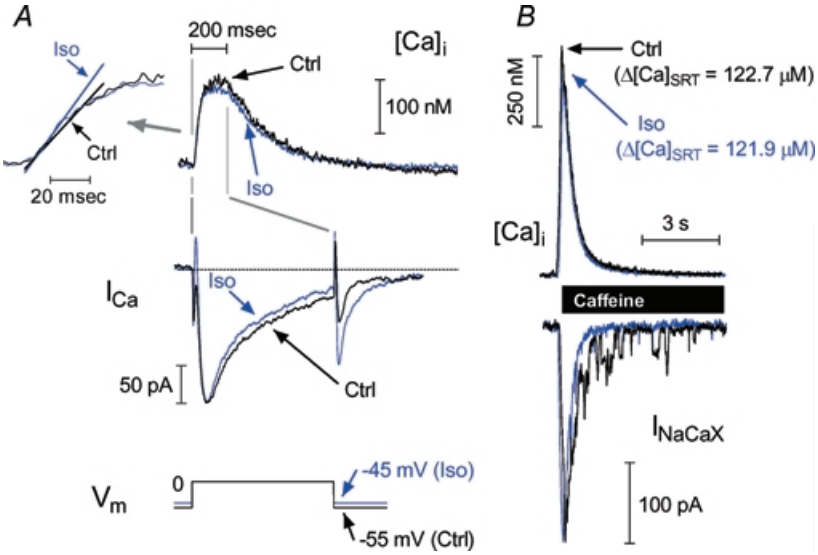

Figure 3. ISO response with I_{Ca} trigger and SR Ca^{2+} load held constant
Example records of $[Ca^{2+}]_i$ and I_{Ca} (*A*) with closely matched I_{Ca} amplitude, from one DM mouse myocyte, in control (black traces) and ISO (blue traces). $[Ca^{2+}]_i$ transient amplitude was unaffected by ISO, but inset (*A*, left) shows that maximum rate of rise of $[Ca^{2+}]_i$ increased. *B*, caffeine-evoked $[Ca^{2+}]_i$ and inward Na^+–Ca^{2+} exchange currents show that SR Ca^{2+} loading was well matched.

inward-going I_{Ca} first crossed the asymptotic value and carried out as far as the time of the corresponding peak twitch $[Ca^{2+}]_i$ transient (dots on traces in Fig. 6*A*).

Fractional SR release was calculated by normalizing fitted predictions to the measured SR Ca^{2+} content (dotted lines in Fig. 6*C* and *D*). Figure 6*E* and *F* show corresponding ECC gain functions (obtained as slopes of the data and curves in Fig. 6*C–D*).

The ordinate in Fig. 6*C* has units of nM, while that in Fig. 6*D* is in μM. Thus the gain function in Fig. 6*E* is in nM × F × A^{-1}, while that in Fig. 6*F* is dimensionless.

Ca^{2+} release in virtually every record increased with increasing trigger in a saturating manner, indicating a decreasing gain (for both free and total [Ca]). Release/gain functions from data like those in Figs 4 and 5 showed very clear systematic changes due to SR Ca^{2+} loading and trigger, respectively (independently of ISO). Thus our method of parameterizing Ca^{2+} release/gain is well suited to detecting any changes due to ISO.

Range and grouping of I_{Ca} and SR loads in control and ISO

As shown in Fig. 7*A*, we grouped attained SR Ca^{2+} loads in three ranges (± ISO), to match their means and to put comparable numbers of functions in each group (see Fig. 7 for values). We might expect Ca^{2+} release to be enhanced with ISO (see Introduction), but this could be obscured if SR loading decreased with ISO. To avoid this possible pitfall, we built the SR load groups so that the mean load in each group was at least as high + ISO as without ISO. Trigger I_{Ca} influxes (peak I_{Ca}) were studied over the range 0.2–15 A F^{-1} while corresponding I_{Ca} integrals were examined over the range 0.3–22 μM (respective *x*-axes in Fig. 6*C* and *D*). These ranges extend well below and above the typical I_{Ca} peak influx (~4 A F^{-1}) during action potentials, which would be of the most physiological interest (Yuan *et al.* 1996).

Amplitude-based Ca^{2+} release and gain were minimally affected by ISO

In Fig. 7 we also show Ca^{2+} transient amplitude (*B*) and total SR Ca^{2+} release (*C*) in the three SR load ranges, for control (thick lines) and ISO (thin lines). Each curve is the average of *n* curves (*n* shown in Fig. 7*A*) for the corresponding load and condition. All release functions saturated, but saturation appeared at higher influxes when SR load was higher. Release increased systematically with increasing load or increasing trigger, and these changes

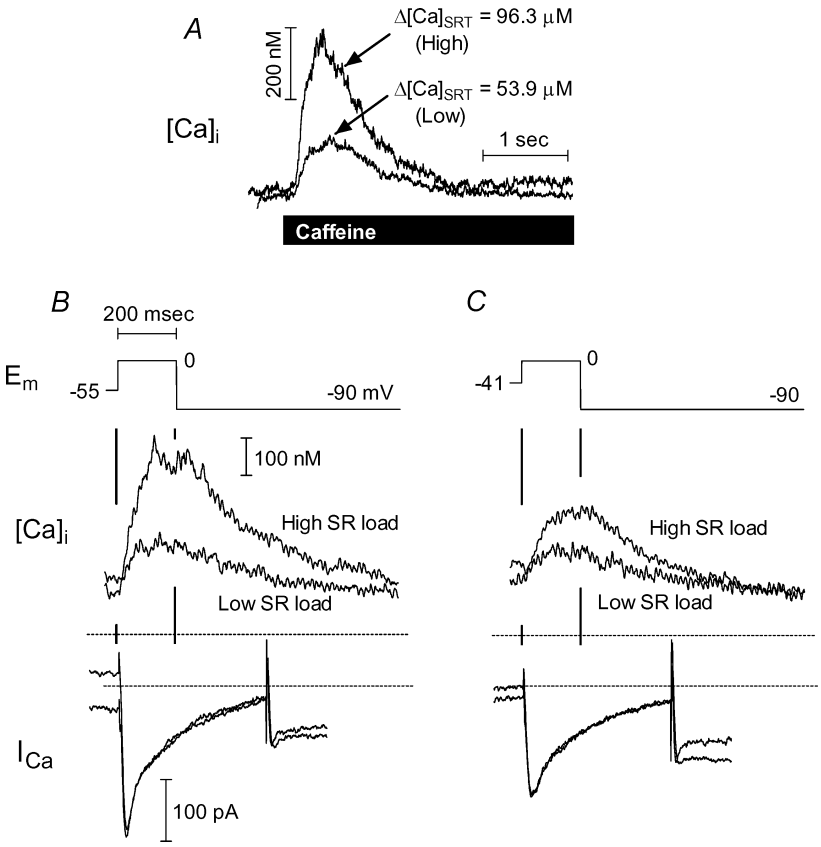

Figure 4. E–C coupling gain increased with SR Ca^{2+} load at constant trigger strength
A, Caffeine-induced $[Ca^{2+}]_i$ transients showing high and low SR loads. Below are responses at the two loads to two trigger strengths, set with either minimal (*B*; V_h = −55 mV) or substantial (*C*; V_h = −41 mV) I_{Ca} pre-inactivation. Rabbit cell, control only. This cell subsequently responded robustly to ISO (not shown).

were greater than any change in release ± ISO within a given load range. The small changes seen with ISO were unsystematic; i.e. for either free or total [Ca], release could be slightly reduced, increased, or unaffected by ISO.

Figure 8 shows fractional SR Ca^{2+} release based on total calcium for high (*A*), medium (*B*) and low (*C*) SR load ranges. Release functions were averaged as in Fig. 7, but each release datum was normalized to its corresponding SR load before being included in the average. Because fractional release overcomes small cell-to-cell variations in SR load and is constrained between 0 and 1, it might reveal ISO effects more sensitively. Fractional release, like absolute increase, saturated at higher influxes with higher SR load, but the fraction at saturation was quite constant near 0.6–0.8 in all cases. Fractional release was either slightly reduced or unaffected by ISO (see also Fig. 12*B*).

Figure 9 shows ECC gain for high (*A*), medium (*B*) and low (*C*) SR load ranges. As expected for saturating Ca^{2+} release, gain was highest for the smallest triggers and decreased toward a limiting value as the trigger increased. This limiting gain increased with increasing SR load. For the smallest triggers in each load range, there was more variation in gain ± ISO. The greater scatter at low I_{Ca} or influx is intrinsic to the definition of the gain (small denominator). Throughout the modest-to-large trigger range gain predictions were unchanged ± ISO. In order to show more clearly how ECC gain depended on SR Ca^{2+} load but not on ISO, Fig. 9*D* shows data from *A*, *B*, and *C* replotted at selected I_{Ca}.

Rate of Ca^{2+} release was faster with ISO

Figure 10*A* shows maximal rates of rise (in μM s^{-1}, mean ± S.E.M., with *n* as shown) for twitches whose rising phase was fitted (as in Fig. 6*A*). With ISO, the maximal rate of rise was ∼50% faster *versus* control in each SR load group (all $P < 0.05$). The maximum rate of rise was faster with increasing SR load (control or ISO). We surmised that this was implicit in larger $\Delta[Ca^{2+}]_i$ transients rising faster. In Fig. 10*B*, we show that the maximal rate of $[Ca^{2+}]_i$ rise normalized to $\Delta[Ca^{2+}]_i$ was relatively constant *versus* SR load, yet was still ≥ 50% faster with ISO.

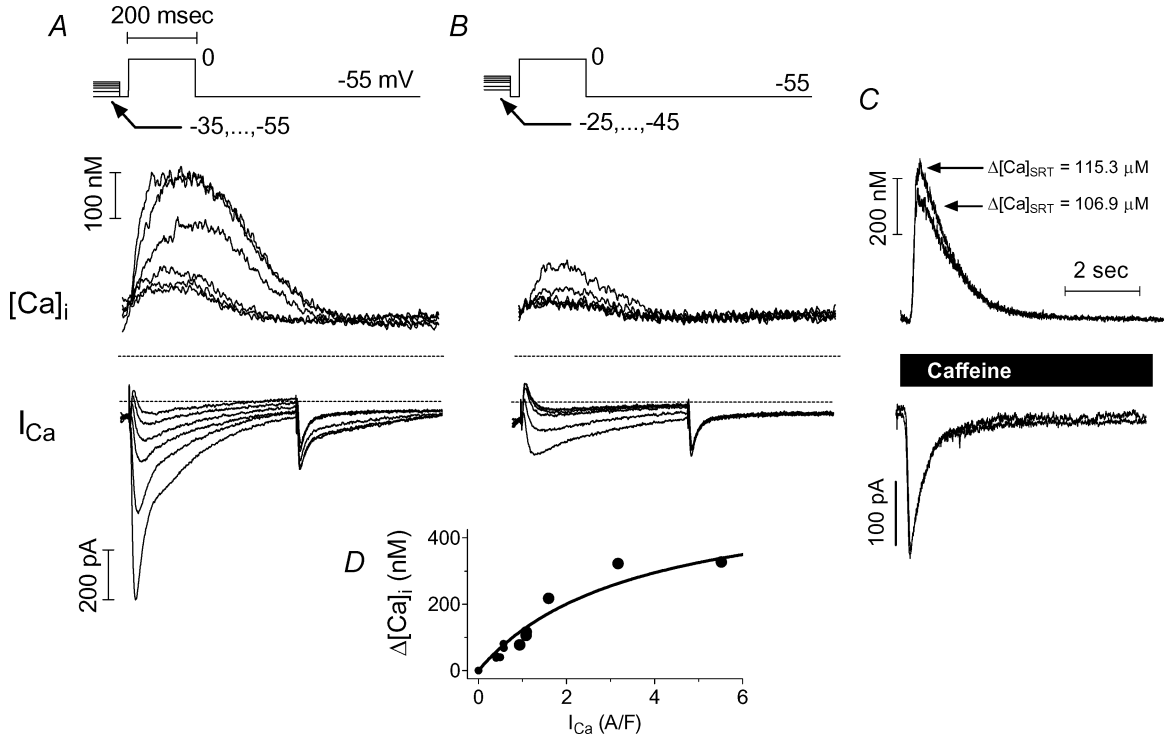

Figure 5. Free Ca^{2+} release increased in graded then saturating fashion with increasing trigger strength at constant SR load

A, $[Ca^{2+}]_i$ transients and I_{Ca} in a larger series generated by pre-inactivating with $V_h = -55$, -47, -42, -39, -36, -33 mV. *B*, $[Ca^{2+}]_i$ transients and I_{Ca} in a smaller series generated by pre-inactivating with $V_h = -45$, -40, -34, -31, -28, -25 mV. *C*, SR loads in the two series matched closely according to $[Ca^{2+}]_i$ transient and I_{NaCaX}. Rabbit cell during ISO treatment. Cell responded robustly on application of ISO (not shown). *D*, both sets of release followed the same functional dependence on I_{Ca}.

We also expected larger I_{Ca} to produce faster rising $\Delta[Ca^{2+}]_i$ transients. In Fig. 10*C* we plot a 'rate gain' measure ($d[Ca^{2+}]_i/dt_{max}/(I_{Ca})$, which also shows that release was faster with ISO. For this figure, to re-express free $d[Ca^{2+}]_i/dt_{max}$ as total, we scaled it up by the approximate cytosolic buffering power for rabbit myocytes (×110; Delbridge *et al.* 1996). Thus, the rate gains here, like the total calcium-based gains in Fig. 9, are dimensionless and

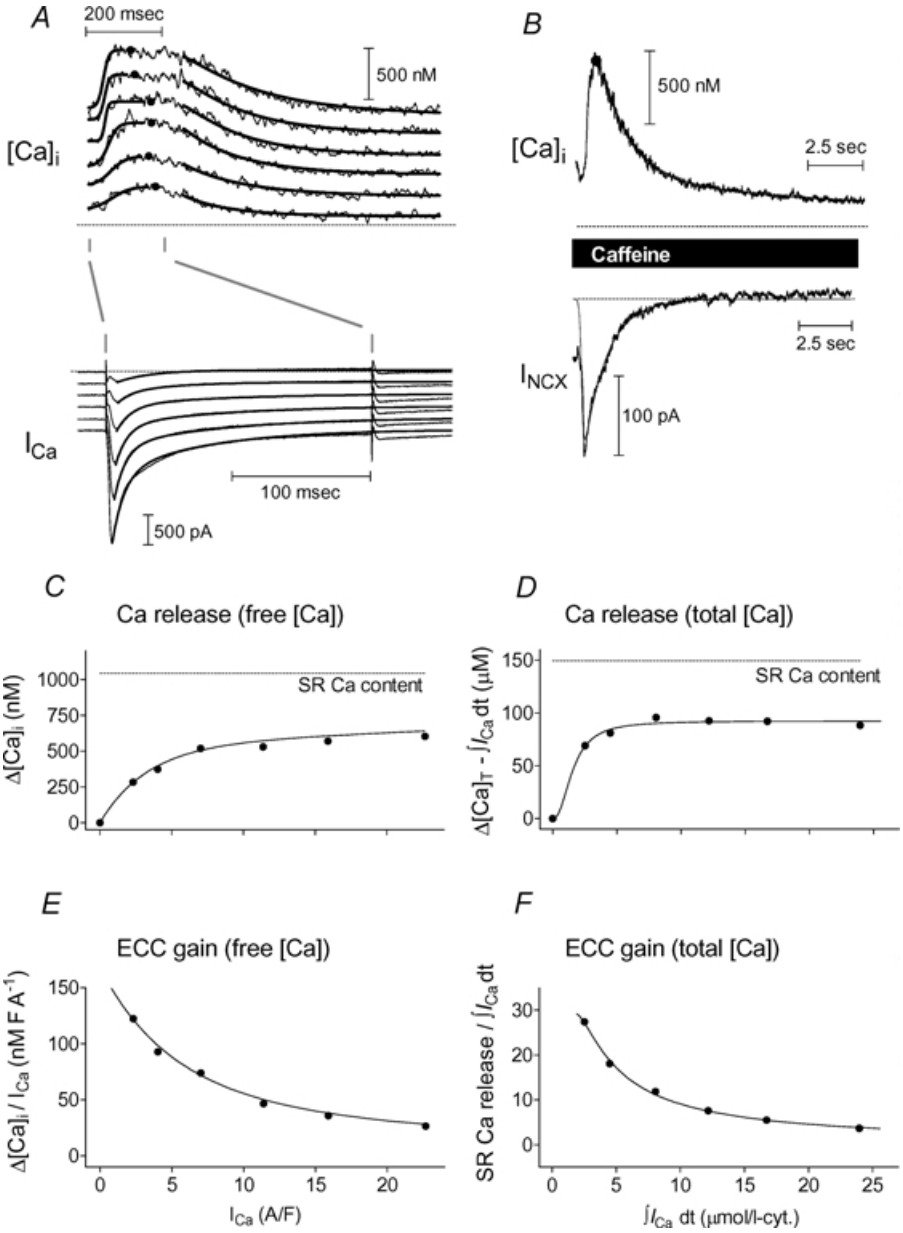

Figure 6. Release and gain functions

A, top, $[Ca^{2+}]_i$ transients and I_{Ca} from a set of 6 twitches associated with a particular conditioned SR Ca^{2+} load. Traces shown separated by 200 pA (I_{Ca}) and 200 nM ($[Ca^{2+}]_i$), respectively, for clarity. $[Ca^{2+}]_i$ peaks and times of peak were found by examination (dots). Maximum rates of rise (with times of occurrence), half-decay times, and a common asymptotic baseline were all found by fitting (bold lines). *A*, bottom, I_{Ca} was similarly fitted with a common asymptote serving as a baseline for amplitude and integral calculations. *B*, corresponding caffeine-evoked $[Ca^{2+}]_i$ (top) and I_{NaCaX} (bottom) were also fitted (same baseline as the twitch $[Ca^{2+}]_i$ in *A*) to establish SR Ca^{2+} load. *C*, Ca^{2+} release data (peak – asymptotic $[Ca^{2+}]_i$) are fitted to allow interpolation or extrapolation to I_{Ca} values not specifically measured. Dotted line indicates SR Ca^{2+} load. *D*, same as *C*, but peak and asymptotic free Ca^{2+} were first converted to total [Ca] and subtracted, and then Ca^{2+} influx (I_{Ca} integral) was removed to find net change in total [Ca]. *E* and *F*, same as *C* and *D*, respectively, with all data converted to gain by expressing release/influx.

amount to small whole numbers, as expected for Ca^{2+}-induced Ca^{2+} release. Finally, in Fig. 10*D* we show that the time from depolarization to maximum release rate was also earlier with ISO. The time-to-peak of I_{Ca} (not shown) did not shorten with ISO and so probably does not explain the faster $\Delta[Ca^{2+}]_i$.

In Fig. 11 appear functions (analogous to the gain functions of Fig. 9) to show how rate gain depended on I_{Ca} for the high (*A*), medium (*B*) and low (*C*) SR load ranges. Rate gain increased systematically with ISO at any SR load, and with increasing load regardless of ISO. Figure 11*D* replots data in *A*, *B*, and *C* at selected I_{Ca}, to show that rate gain increased dramatically for small I_{Ca}, increased somewhat with increasing SR load, and increased systematically with ISO.

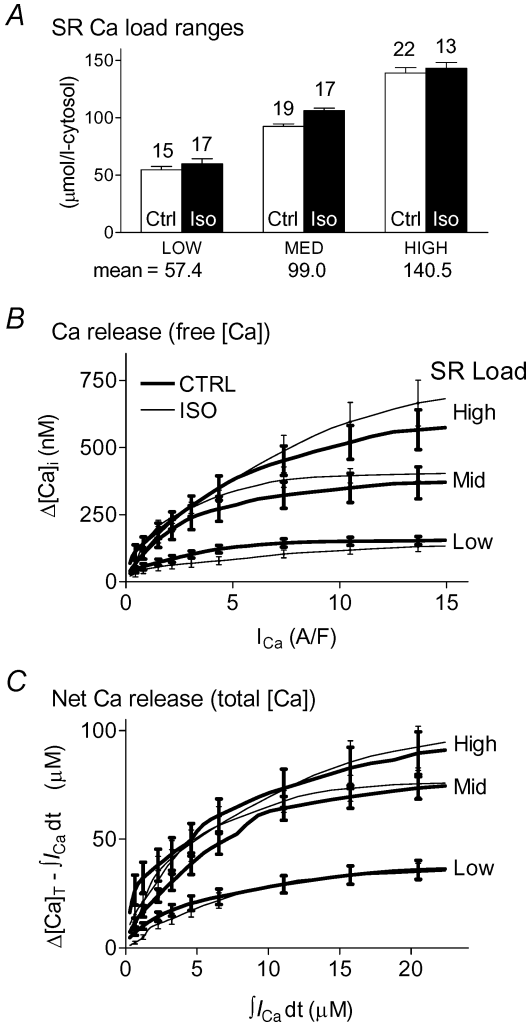

Figure 7. Ca^{2+} release amplitude did not change with ISO
A, classification of SR load data in three overlapping ranges ± ISO. Load group boundaries were set to give comparable mean values and numbers of observations in each group. *B* and *C*, Ca^{2+} release functions expressed as free $\Delta[Ca^{2+}]_i$ (*B*) and total $\Delta[Ca]_T$ (*C*) increased with trigger in saturating fashion, and also increased with SR load. ISO affected free Ca^{2+} release minimally and unsystematically, especially compared with effects of trigger and load themselves. Each trace is the average of predictions made for the available data in a given load range (*n* shown in Fig. 7*A*). Error bars (± S.E.M.) were placed at visually convenient intervals.

Rates of I_{Ca} and $[Ca^{2+}]_i$ decline with ISO

Faster SR Ca^{2+} release should accelerate I_{Ca} inactivation (Bers, 2001). Figure 12*A* shows that ISO slightly but significantly accelerated the fast component of I_{Ca} decay rate, without affecting the slow component or the relative strength of the components. Faster I_{Ca} inactivation could contribute to faster shut-off of SR Ca^{2+} release in ISO, an implicit conclusion in our results (i.e. faster Ca^{2+} release rate, but with same integral).

Faster SR Ca^{2+} uptake with ISO could also curtail the peak of the Ca^{2+} transient, resulting in an underestimation of the total SR Ca^{2+} release in ISO (Bassani *et al.* 1994). Indeed $[Ca^{2+}]_i$ decay was faster with ISO in rabbit, though

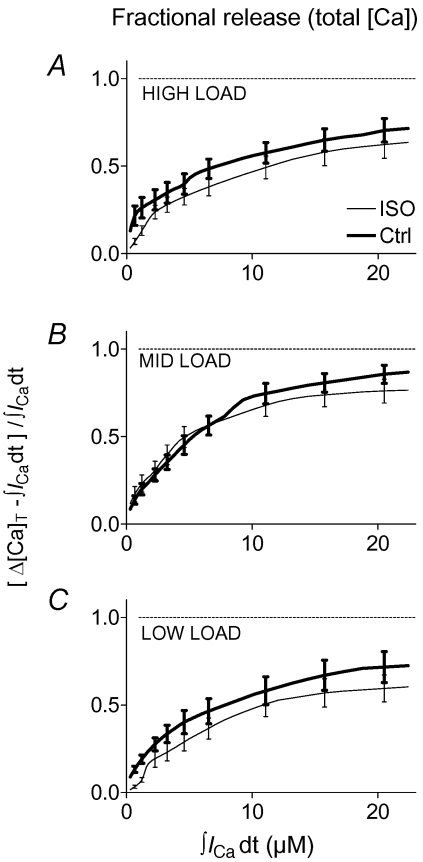

Figure 8. Fractional Ca^{2+} release did not change with ISO
The predictions of Fig. 7*B* for total calcium release are shown converted to a fraction of the SR Ca^{2+} load released, to help separate the ISO effect from the load-dependent effect. Under either condition (control or ISO), fractional release saturated near 0.7.

much less so in mouse (Figs 2 and 3), even if we studied only similar-sized $\Delta[Ca^{2+}]_i$ and I_{Ca} ± ISO to remove intrinsic effects of amplitude on τ (Bers & Berlin, 1995; not shown). In Fig. 8, fractional SR Ca^{2+} release + ISO for large triggers fell slightly below release without ISO. This might represent a slight snubbing of peak $[Ca^{2+}]_i$ by faster SR Ca^{2+} uptake, particularly when released $[Ca^{2+}]$ was large. To test this we plotted fractional SR Ca^{2+} release data (all SR loads) separately for rabbit and mouse (Fig. 12*B*). Indeed, fractional SR Ca^{2+} release was slightly lower with ISO in rabbit but not in mouse, where SR Ca^{2+} uptake was not affected (Brittsan *et al.* 2003) consistent with our conclusion that SR Ca^{2+} release amplitude is stable ± ISO.

Discussion

Rationale

The inotropic effect of sympathetic stimulation of the heart is mediated mainly by β-AR and PKA activation (Bers, 2001). There are four main PKA targets affecting ECC: I_{Ca}, PLB, TnI and RyR. There is extensive and compelling evidence that PKA increases I_{Ca} and SR Ca^{2+}-ATPase activity (via PLB phosphorylation), and that these two mechanisms contribute centrally to PKA-induced cardiac inotropy.

The functional role of RyR phosphorylation by PKA is more controversial. It has been difficult to isolate RyR function in the cellular environment where I_{Ca} and SR Ca^{2+} load critically determine RyR behaviour and are both altered by PKA. Indeed PKA effects on ECC consistent with increased, decreased and unchanged RyR activation by Ca^{2+} have all been reported in myocyte studies (Viatchenko-Karpinski & Györke, 2001; Song *et al.* 2001; delPrincipe *et al.* 2001; Li *et al.* 2002). Even for isolated RyRs in lipid bilayers, results of PKA phosphorylation are mixed (Valdivia *et al.* 1995; Marx *et al.* 2000; Jiang *et al.* 2002).

Summary of outcome

This study addressed the above problem by comparing SR Ca^{2+} release (± 1 μM ISO) where both I_{Ca} and SR Ca^{2+} load were controlled and measured over a broad range. We found that for any given SR Ca^{2+} load and I_{Ca}, the amount of SR Ca^{2+} release was not significantly affected by ISO (Figs 3, 7 and 9), despite clearly demonstrated ISO effects in the same cells when I_{Ca} and load were not controlled (Fig. 2). This was true whether release amplitude was measured using free Ca^{2+} ($\Delta[Ca^{2+}]_i$; Fig. 7*B*), total calcium ($\Delta[Ca]_T$; Fig. 7*C* and 9), or fractional SR Ca^{2+} release (Fig. 8), and whether expressed directly (Figs 7*B* and *C*) or using ECC gain functions (SR Ca^{2+} released–integrated I_{Ca}; Fig. 9). In contrast, I_{Ca} and SR Ca^{2+} load specifically and strongly affected Ca^{2+} release and gain, independently of ISO (Figs 4 and 5).

Despite not altering the overall amount of Ca^{2+} released, ISO did systematically increase the maximal rate of SR Ca^{2+} release for a given I_{Ca} and SR Ca^{2+} load (Figs 10 and 11). Since release amplitude was constant, some means must also hasten the turn-off of Ca^{2+} release when ISO is present.

Control of I_{Ca} and SR Ca^{2+} uptake and loading

Increasing either I_{Ca} or SR Ca^{2+} load increases SR Ca^{2+} release (Fabiato, 1983; Bers, 2001; Figs 4 and 5). The

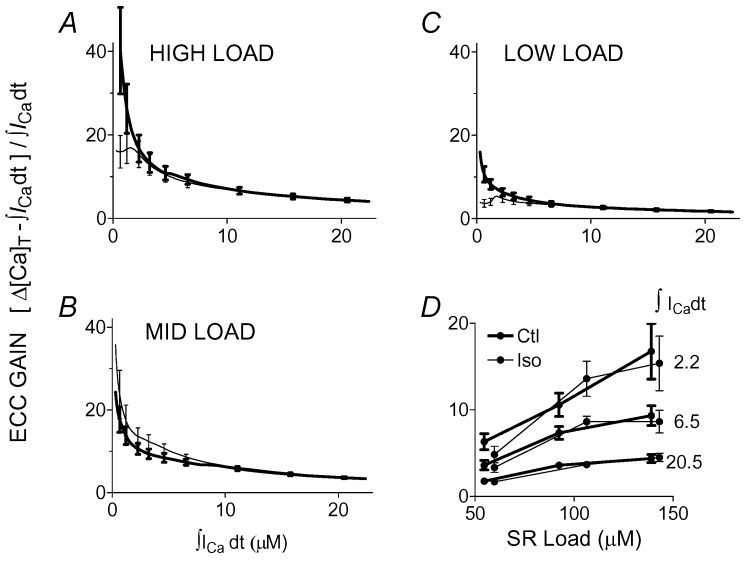

Figure 9. ECC gain did not change with ISO
The predictions of Fig. 7*C* have been converted to gain and are shown separately for high (*A*), medium (*B*) and low (*C*) SR load ranges. Each release datum was divided by the corresponding influx. At very large triggers, saturation of release left gain at its smallest and least sensitive to modulation, while small and unsystematic effects are seen in the smallest trigger ranges. *D*, predictions at three selected Ca^{2+} influxes are replotted to show that gain increased with increasing SR Load.

ability of I_{Ca} to control SR Ca^{2+} release (at constant SR Ca^{2+} load) in graded fashion is at the heart of the CICR mechanism. At the same time, the relationship between SR Ca^{2+} load and SR Ca^{2+} release is very steep, so that small changes in SR Ca^{2+} load can greatly alter SR Ca^{2+} release. To accomplish the required control of both I_{Ca} and SR Ca^{2+} load (measured almost cotemporally with each set of twitches), several options were available.

We varied I_{Ca} by altering Ca^{2+} channel availability (Fig. 1), rather than test E_m or $[Ca^{2+}]_o$. ISO enhances macroscopic I_{Ca} mostly by increasing channel open probability. Our use of pre-inactivation with ISO present compensated properly for this by reducing the number of channels available. Indeed, if we had altered test E_m or $[Ca^{2+}]_o$, we would have altered single channel I_{Ca} and latency (with consequent effects on ECC gain; see below). We believe that single channel I_{Ca} would not vary in our protocol.

Despite this, ISO also can promote long (mode 2) L-type Ca^{2+} channel openings (Yue *et al.* 1990). For a given macroscopic I_{Ca}, if mode 2 openings occur, then fewer channels must be active. If the initial part of an I_{Ca} opening is what triggers SR Ca^{2+} release, Ca^{2+} admitted later during prolonged openings would be largely wasted, appearing to decrease ECC gain, i.e. there would be less SR Ca^{2+} release for a given I_{Ca}. Indeed, Ca^{2+} channel agonists such as BayK-8644 (Tsien *et al.* 1986) or FPL-64176 (Janczewski *et al.* 2000), which strongly promote mode 2 behaviour, do reduce Ca^{2+} release and intrinsic ECC gain (McCall & Bers, 1996). We think mode 2 openings are not a complication in our experiments because unlike BayK-8644 or FPL-64176, ISO increases I_{Ca} primarily by promoting channel availability, with mode 2 openings being quite rare (Hirano *et al.* 1999).

Increased SR Ca^{2+} content enhances RyR-mediated SR Ca^{2+} release by directly increasing driving force and through allosteric increase of P_o (Han *et al.* 1994; Sitsapesan & Williams, 1994; Györke & Györke, 1998; Bassani *et al.* 1995*b*; Shannon *et al.* 2000; Eisner *et al.* 2000). Thus controlling for SR Ca^{2+} load as shown in Fig. 7*A* is an absolute requirement for measuring the independent effects of PKA on RyR function in intact cells.

Even with load controlled, PLB phosphorylation by PKA could complicate our study by accelerating SR Ca^{2+} reuptake, which could curtail the peak $[Ca^{2+}]_i$ transient (Bassani *et al.* 1994). This complication was controlled

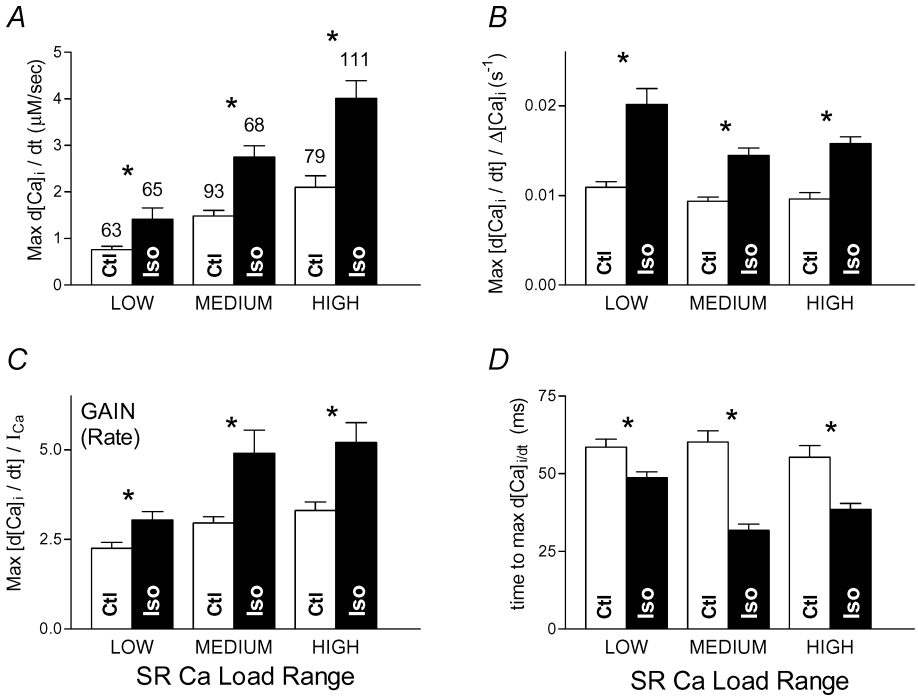

Figure 10. Temporal properties of Ca^{2+} transients with ISO
A, maximal rate of rise of $[Ca^{2+}]_i$ transients was substantially faster with ISO. Maximal rate of rise was also faster with increased SR loading, but this may be explained by the larger sizes of $[Ca^{2+}]_i$ transients, as shown in *B* (data of *A* normalized to $[Ca^{2+}]_i$ amplitude). *C*, 'Rate gain', i.e. maximal rate of rise normalized to I_{Ca} peak influx rate, was also higher with ISO. *D*, time at which maximal rate of rise (*A*) occurred was earlier with ISO. All comparisons: $^*P < 0.05$.

for in the experiments with transgenic mice expressing only non-phosphorylatable PLB. As shown in Figs 3 and 12*B*, ISO did not affect Ca^{2+} release in the mouse model. Although a slight loss of fractional SR Ca^{2+} release with ISO was evident in rabbit *versus* mouse (Fig. 12*B*), no rabbit *versus* mouse differences were evident when the analyses in Figs 7*B*, *C* and 9 were repeated separately for rabbit and mouse (not shown).

Fractional SR Ca^{2+} release and ECC gain

Two complementary numerical indices of cardiac ECC efficacy are in common use: fractional SR Ca^{2+} release and ECC gain. Both are useful, but neither can completely describe ECC efficacy because they depend on both Ca^{2+} influx and SR load. In this study, for both SR Ca^{2+} release and ECC gain (in absolute and in dimensionless units), we have made explicit these functional dependencies. Both Ca^{2+} release and gain increase with increasing SR Ca^{2+} load but depend more complexly on I_{Ca} (see below).

The fact that our analyses (and choice of experimental conditions) effectively reproduce the known specific dependency of Ca^{2+} release and ECC gain on trigger and SR load shows that they are robust enough to support our conclusions.

Increasing ECC gain for small I_{Ca}

Most previous studies of ECC gain have used test E_m to vary I_{Ca} (e.g. López-López *et al.* 1994; Wier *et al.* 1994; Cannell *et al.* 1995; Santana *et al.* 1996). These studies demonstrated that ECC gain increased as I_{Ca} amplitude was reduced by increasingly negative test E_m. The higher gain at smaller I_{Ca} was attributed mainly to the higher single channel I_{Ca} expected at more negative E_m, due to higher electrochemical driving force. Our observation that ECC gain increased with smaller I_{Ca} at constant E_m (smaller probability of opening, but constant unitary I_{Ca} amplitude; Figs 6 and 9) indicates that this cannot be the entire explanation. Our working hypothesis is that the reduction in ECC gain at higher I_{Ca} amplitude is largely due to redundant Ca^{2+} channel opening at a single SR Ca^{2+} release site. That is, a single Ca^{2+} channel opening may be sufficient to activate a whole cluster of RyRs at a

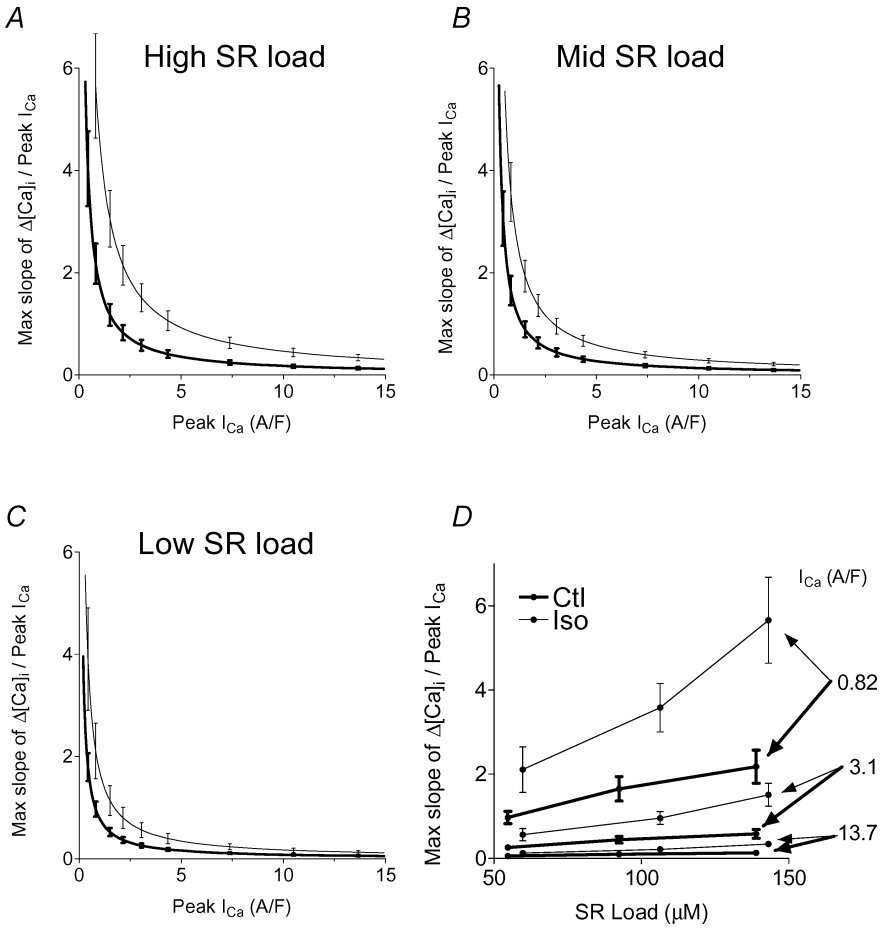

Figure 11. Ca^{2+} release normalized to influx was faster with ISO
'Rate gain', i.e. maximal rate of rise normalized to I_{Ca} peak influx rate, increased with increasing SR load (*A*, *B* and *C*), and decreased with increasing Ca^{2+} influx, but was systematically higher with ISO. *D*, predictions at three selected Ca^{2+} influxes are replotted to show that rate gain increased with increasing SR load and decreased dramatically with increasing trigger.

single junction, via CICR (Santana *et al.* 1996). Additional L-type Ca^{2+} channel openings at the same junction would increase I_{Ca} but not increase release. Thus the ECC gain denominator (I_{Ca}) would rise for the same numerator. A relatively high fidelity of triggered release (Inoue & Bridge, 2003) is consistent with data suggesting that there are ~10–20 L-type Ca^{2+} channels at a single junction associated with ~100 RyRs (Bers & Stiffel, 1993; Franzini-Armstrong *et al.* 1999). Thus increasing unitary I_{Ca} may be only a minor factor in ECC gain increase at negative E_m, and the likelihood of high Ca^{2+} channel opening probabilities producing redundant Ca^{2+} influx at more moderate E_m needs to be considered.

ECC gain continues to decline monotonically at more positive test E_m (> +20 mV) as I_{Ca} becomes smaller again. At these positive E_m virtually all available Ca^{2+} channels will be activated, so the redundancy effect to reduce ECC gain would already be maximal. The decrease in unitary I_{Ca} as E_m approaches the I_{Ca} reversal potential may then more critically limit ECC fidelity and gain in that E_m region. This is functionally important, because physiological SR Ca^{2+} release occurs during the early phases of the action potential where E_m is +20 to +50 mV.

Another factor which could affect E_m dependence of ECC gain is the I_{Ca} first latency, which would be most variable at small depolarizations (Rose *et al.* 1992), reducing fidelity and possibly gain by inducing more variability in kinetics and spatial uniformity of SR Ca^{2+} release.

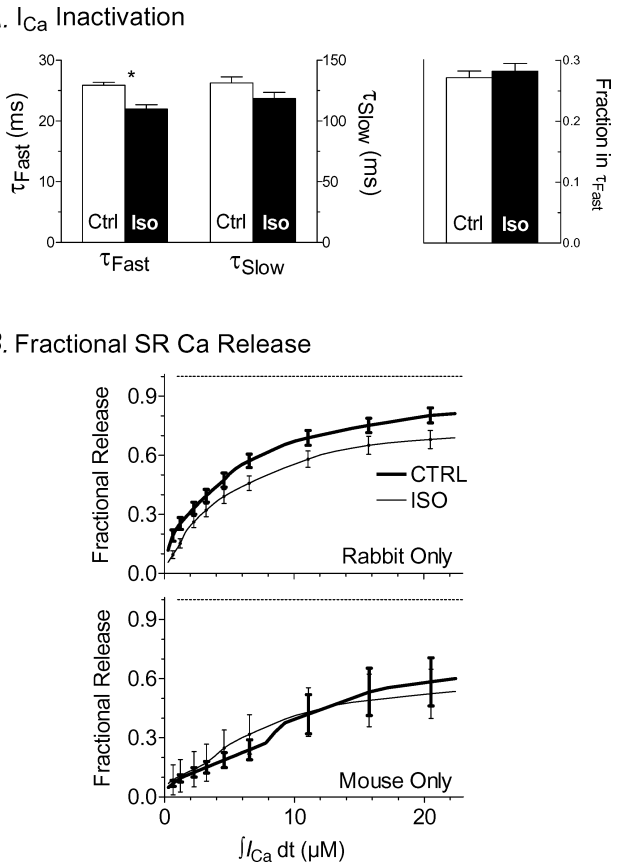

Figure 12. I_{Ca} inactivation and species dependence of fractional SR Ca^{2+} release

A, I_{Ca} decline was fitted to a biexponential function; the fast decay time constant τ_{fast} shortened with ISO, but τ_{slow} and the proportion of amplitude in the fast component did not change. *B*, fractional SR Ca^{2+} release data from Fig. 9, separated by species (including all SR Ca^{2+} load groups), shows constancy of release ± ISO in mouse.

Relationship to previous results

Single isolated cardiac RyRs in lipid bilayers have yielded mixed results with PKA phosphorylation. Valdivia *et al.* (1995) found that RyR P_o decreased with PKA activation at resting [Ca^{2+}], while the measured RyR response to rapid jumps in [Ca^{2+}] meant to simulate cellular I_{Ca} was an initially high P_o that relaxed back to a lower steady-state level, still exceeding that before [Ca^{2+}] was elevated. This pattern is consistent with our cellular results.

Marx *et al.* (2000) studied only steady-state P_o of single RyRs and found that PKA increased open probability, but also revealed reduced unitary conductance sub-states. Similar subconductance states were observed after depleting FK-506 binding protein (FKBP) from the RyR (Kaftan *et al.* 1996) and further, PKA could cause FKBP to dissociate from RyR (Marx *et al.* 2000). Some of these observations were not confirmed by Jiang *et al.* (2002).

Marx *et al.* (2000) inferred that PKA phosphorylation would cause a net increase in Ca^{2+} release, consistent with our observed faster initial release. Increased RyR P_o may in time be counterbalanced by reduced conductance, leaving little or no net effect on release. Independently of RyR properties, enhanced I_{Ca} inactivation and/or SR Ca^{2+} uptake could also stabilize ECC gain with ISO in the intact cell (Fig. 12), but SR uptake (as relaxation rate) was unchanged in our mouse data.

Previously we showed that PKA-dependent phosphorylation of the RyR had no effect on any of frequency, kinetic or spatial properties of Ca^{2+} sparks in intact or permeabilized ventricular myocytes under diastolic conditions, provided that SR Ca^{2+} load and $[Ca^{2+}]_i$ were unaltered (Li *et al.* 2002). We confirmed that elevating cytosolic [Ca^{2+}] or SR Ca^{2+} load potently increased Ca^{2+} spark frequency. This is consistent with our finding of no effect of PKA on amplitude-based measures of Ca^{2+} release here and the modest resting state

depression of RyR P_o by PKA described by Valdivia *et al.* (1995).

In intact ventricular myocytes, ISO increased Ca^{2+} release during ECC (Hussain & Orchard, 1997), but this could be attributed to increased SR load and I_{Ca}. The bell-shaped trigger voltage dependence of Ca^{2+} release became flat-topped with ISO but reappeared if conditioning was adjusted to reduce SR Ca^{2+} load or if trigger strength was reduced with nifedipine. This emphasizes the importance of controlling I_{Ca} and SR Ca^{2+} load in assessing the independent effect of RyR phosphorylation on ECC.

Viatchenko-Karpinski & Györke (2001) found that ISO modestly increased SR Ca^{2+} release and ECC gain (as $(\Delta F/F_o)$/peak (I_{Ca}), but they did not make gain comparisons where I_{Ca} was the same (nor did they measure Ca^{2+} release rates). They did find comparable SR Ca^{2+} loading ± ISO, but this was not measured in the same cells or conditions as ECC gain. PKA activation increased ECC gain only when Na^+ was present in pipette and bath, not under Na^+-free conditions. Possibly internal Na^+ promoted Ca^{2+} influx via Na^+–Ca^{2+} exchange, not accounted for in I_{Ca}, which could lower threshold, increase SR loading, and/or increase spatial spread of triggering and released Ca^{2+} among release units. Our use of Na^+-free pipettes and keeping I_{Na} inactivated prevented Ca^{2+} influx via Na^+–Ca^{2+} exchange.

In a preliminary report delPrincipe *et al.* (2001) found that PKA activation increased SR Ca^{2+} release in response to a flash-photolysis-evoked Ca^{2+} trigger. In this case the Ca^{2+} trigger may be more alike (± PKA), but it is unlike the spatially focused physiological I_{Ca} trigger.

Song *et al.* (2001) reported that PKA activation decreased ECC gain (based on Ca^{2+} release rates measured as Ca^{2+} spikes with millimolar cytosolic Ca^{2+} buffering). This outcome, under conditions which should emphasize changes in initial release rate, contradicts our finding of faster release. Their reduction in gain was only seen for $E_m = 0$ mV, not at positive E_m. In Song *et al.* (2001), I_{Ca} triggers were relatively large and not specifically matched ± PKA activation. Without specific matching, ISO data would fall along a more saturated part (larger I_{Ca} *versus* control data) of a possibly unchanged ECC gain *versus* trigger function.

Earlier termination of Ca^{2+} release with ISO

RyR gating is sensitive to intra-SR free $[Ca^{2+}]$ (Sitsapesan & Williams, 1994; Györke & Györke, 1998; Bassani *et al.* 1995*a*; Shannon *et al.* 2000). Moreover, in direct measurements of intra-SR free $[Ca^{2+}]$, Shannon *et al.* (2003) showed that SR Ca^{2+} release appears to turn off robustly when SR $[Ca^{2+}]$ drops only partially (e.g. to ~0.4 mM), regardless of initial SR Ca^{2+} load. With ISO, the faster initial release would then lead intra-SR free $[Ca^{2+}]$ to fall earlier to the threshold for termination, which could explain the lack of effect of ISO on the total amount released.

Contrasting PKA *versus* CaMKII effects on SR Ca^{2+} release and ECC gain

CaMKII can also modify RyR gating in lipid bilayers, but as with PKA phosphorylation the results are mixed, with increases and decreases in P_o reported (Witcher *et al.* 1991; Hain *et al.* 1995; Lokuta *et al.* 1995). We previously studied the effect of CaMKII activation on RyR function in intact ventricular myocytes, using a similar approach to that used here (Li *et al.* 1997). Activation of endogenous CaMKII during conditioning pulses dramatically increased fractional SR Ca^{2+} release and ECC gain (when both I_{Ca} and SR Ca^{2+} load were well matched before and after). In transgenic mice overexpressing the cytosolic form of cardiac CaMKII we found dramatic activation of Ca^{2+} spark frequency (despite lower SR Ca^{2+} load and diastolic $[Ca^{2+}]_i$) which was acutely reversed by inhibition of CaMKII by KN-93 (Maier *et al.* 2003). Twitch fractional Ca^{2+} release was also increased in these mice, despite lower SR load (which normally depresses fractional release). These strong CaMKII effects on intact-cell RyR function contrast strikingly with our present study where PKA activation did not appreciably alter these parameters.

The strong CaMKII effect of increasing ECC efficacy shows that changes in RyR function are in principle detectable in intact cells using experimental designs like ours and that of Li *et al.* (1997). More importantly, our finding that Ca^{2+} release was faster but unchanged in strength with PKA may point to a general contrast between PKA and CaMKII phenomena (which may have a basis in the ability of CaMKII to phosphorylate sites on RyR not phosphorylated by PKA; Rodriguez *et al.* 2003). PKA and β-AR activation seem generally to hasten intact cardiac cellular responses (e.g. faster onset and relaxation of contraction, faster Ca^{2+} removal/uptake, faster pacemaker rate, action potential propagation and repolarization) while CaMKII activation may intensify them.

Conclusion – physiological implications

When I_{Ca} and SR Ca^{2+} load were controlled, we could detect no effect of ISO on amplitude-based measures of ECC efficacy (absolute or fractional SR Ca^{2+} release or ECC gain) over a broad range of I_{Ca} and load values.

However, PKA activation increased the maximal rate of $[Ca^{2+}]_i$ rise (and ECC gain based on that) by nearly 50%. This outcome, considered along with the contrasting effect of CaMKII activation to increase Ca^{2+} release strength but not necessarily kinetics, may be part of a general pattern of PKA responses, where fight or flight transient behaviour is crucial (Marks, 2003).

'Coordinated control' of ECC has been proposed, where interventions expected to modulate RyR function affected ECC only transiently, due to feedback autoregulation of Ca^{2+} influx and SR loading (Díaz *et al.* 2000; Eisner & Trafford, 2000). While coordinated control could stabilize ECC with PKA activation in the intact setting, we have disabled this feedback path by specifically controlling Ca^{2+} influx and loading.

References

Bassani JWM, Bassani RA & Bers DM (1994). Relaxation in rabbit and rat cardiac cells: species-dependent differences in cellular mechanisms. *J Physiol* **476**, 279–293.

Bassani JWM, Bassani RA & Bers DM (1995*a*). Calibration of indo-1 and resting intracellular $[Ca]_i$ in intact rabbit cardiac myocytes. *Biophys J* **68**, 1453–1460.

Bassani JWM, Yuan W-L & Bers DM (1995*b*). Fractional SR Ca release is regulated by trigger Ca and SR Ca content in cardiac myocytes. *Am J Physiol* **268**, C1313–C1319.

Bean BP, Nowycky MC & Tsien RW (1984). β-Adrenergic modulation of calcium channels in frog ventricular heart cells. *Nature* **307**, 371–375.

Bers DM (2001). *Excitation-Contraction Coupling and Cardiac Contractile Force*. Kluwer, Dordrecht, The Netherlands.

Bers DM & Berlin JR (1995). Kinetics of $[Ca]_i$ decline in cardiac myocytes depend on peak $[Ca]_i$. *Am J Physiol* **268**, C271–C277.

Bers DM & Stiffel VM (1993). Ratio of ryanodine to dihydropyridine receptors in cardiac and skeletal muscle and implications for E-C coupling. *Am J Physiol* **264**, C1587–C1593.

Brittsan AG, Ginsburg KS, Chu G, Yatani A, Wolska BM, Schmidt AG, Asahi M, MacLennan DH, Bers DM & Kranias EG (2003). Chronic SR Ca^{2+}-ATPase inhibition causes adaptive changes in cellular Ca^{2+} transport. *Circ Res* **92**, 769–776.

Callewaert G, Cleemann L & Morad M (1988). Epinephrine enhances Ca^{2+} current-regulated Ca^{2+} release and Ca^{2+} reuptake in rat ventricular myocytes. *Proc Natl Acad Sci U S A* **85**, 2009–2013.

Cannell MB, Cheng H & Lederer WJ (1995). The control of calcium release in heart muscle. *Science* **268**, 1045–1049.

Cheng H, Lederer WJ & Cannell MB (1993). Calcium sparks: elementary events underlying excitation-contraction coupling in heart muscle. *Science* **262**, 740–744.

Delbridge LM, Bassani JWM & Bers DM (1996). Steady-state twitch Ca^{2+} fluxes and cytosolic Ca^{2+} buffering in rabbit ventricular myocytes. *Am J Physiol* **270**, C192–C199.

delPrincipe F, Egger M, Pignier C & Niggli E (2001). Enhanced E-C coupling efficiency after Beta-stimulation of cardiac myocytes. *Biophys J* **80**, 64a.

Díaz ME, Trafford AW, O'Neill SC & Eisner DA (2000). Can changes of ryanodine receptor expression affect cardiac contractility? *Cardiovasc Res* **45**, 1068–1071.

Eisner DA, Choi HS, Diaz ME, O'Neill SC & Trafford AW (2000). Integrative analysis of calcium cycling in cardiac muscle. *Circ Res* **87**, 1087–1094.

Eisner DA & Trafford AW (2000). No role for the ryanodine receptor in regulating cardiac contraction? *News Physiol Sci* **15**, 275–279.

Elliott TR (1905). The action of adrenalin. *J Physiol* **32**, 401–467.

Fabiato A (1983). Calcium-induced release of calcium from the cardiac sarcoplasmic reticulum. *Am J Physiol* **245**, C1–C14.

Franzini-Armstrong C, Protasi F & Ramesh V (1999). Shape size, and distribution of Ca^{2+} release units and couplons in skeletal and cardiac muscles. *Biophys J* **77**, 1528–1539.

Ginsburg KS, Weber CR & Bers DM (1998). Control of maximum sarcoplasmic reticulum Ca load in intact ferret ventricular myocytes. Effects of thapsigargin and isoproterenol. *J General Physiol* **111**, 491–504.

Grynkiewicz G, Poenie M & Tsien RY (1985). A new generation of Ca indicators with greatly improved fluorescence properties. *J Biol Chem* **260**, 3440–3450.

Györke I & Györke S (1998). Regulation of the cardiac ryanodine receptor channel by luminal Ca^{2+} involves luminal Ca^{2+} sensing sites. *Biophys J* **75**, 2801–2810.

Hain J, Onoue H, Mayrleitner M, Fleischer S & Schindler H (1995). Phosphorylation modulates the function of the calcium release channel of sarcoplasmic reticulum from cardiac muscle. *J Biol Chem* **270**, 2074–2081.

Han S, Schiefer A & Isenberg G (1994). Ca^{2+} load of guinea-pig ventricular myocytes determines efficacy of brief Ca^{2+} currents as trigger for Ca^{2+} release. *J Physiol* **480**, 411–421.

Hirano Y, Yoshinaga T, Murata M & Hiraoka M (1999). Prepulse-induced mode 2 gating behavior with and without beta-adrenergic stimulation in cardiac L-type Ca channels. *Am J Physiol* **276**, C1338–C1345.

Hove-Madsen L & Bers DM (1993). Passive Ca buffering and SR Ca uptake in permeabilized rabbit ventricular myocytes. *Am J Physiol* **264**, C677–C686.

Hussain M & Orchard CH (1997). Sarcoplasmic reticulum Ca^{2+} content, L-type Ca^{2+} current, and the Ca^{2+} transient in rat myocytes during β-adrenergic stimulation. *J Physiol* **505**, 385–402.

Inoue M & Bridge JH (2003). Ca^{2+} sparks in rabbit ventricular myocytes evoked by action potentials: involvement of clusters of L-type Ca^{2+} channels. *Circ Res* **92**, 532–538.

Janczewski AM, Lakatta EG & Stern MD (2000). Voltage-independent changes in L-type Ca^{2+} current uncoupled from SR Ca^{2+} release in cardiac myocytes. *Am J Physiol* **279**, H2024–H2031.

Jiang MT, Lokuta AJ, Farrell EF, Wolff MR, Haworth RA & Valdivia HH (2002). Abnormal Ca2+ release, but normal ryanodine receptors, in canine and human heart failure. *Circ Res* **91**, 1015–1022.

Kaftan E, Marks AR & Ehrlich BE (1996). Effects of rapamycin on ryanodine receptor Ca2+-release channels from cardiac muscle. *Circ Res* **78**, 990–997.

Li Y, Kranias EG, Mignery GA & Bers DM (2002). Protein kinase A phosphorylation of the ryanodine receptor does not affect calcium sparks in mouse ventricular myocytes. *Circ Res* **90**, 309–316.

Li L, Satoh H, Ginsburg KS & Bers DM (1997). The effects of CaMKII on cardiac excitation-contraction coupling in ferret ventricular myocytes. *J Physiol* **501**, 17–32.

Lindemann JP, Jones LR, Hathaway DR, Henry BG & Watanabe AM (1983). β-Adrenergic stimulation of phospholamban phosphorylation and Ca^{2+}-ATPase activity in guinea pig ventricles. *J Biol Chem* **258**, 464–471.

Litwin SE, Li J & Bridge JH (1998). Na-Ca exchange and the trigger for sarcoplasmic reticulum Ca release: studies in adult rabbit ventricular myocytes. *Biophys J* **75**, 359–371.

Lokuta AJ, Rogers TB, Lederer WJ & Valdivia HH (1995). Modulation of cardiac ryanodine receptors of swine and rabbit by a phosphorylation-dephosphorylation mechanism. *J Physiol* **487**, 609–622.

López-López JR, Shacklock PS, Balke CW & Wier WG (1994). Local stochastic release of Ca^{2+} in voltage-clamped rat heart cells: Visualization with confocal microscopy. *J Physiol* **480**, 21–29.

Luo W, Grupp IL, Harrer J, Ponniah S, Grupp G, Duffy JJ, Doetschman T & Kranias EG (1994). Targeted ablation of the phospholamban gene is associated with markedly enhanced myocardial contractility and loss of beta-agonist stimulation. *Circ Res* **75**, 401–409.

McCall E & Bers DM (1996). BAY K 8644 depresses excitation-contraction coupling in cardiac muscle. *Am J Physiol* **270**, C878–C884.

Maier LS, Zhang T, Chen L, DeSantiago J, Brown JH & Bers DM (2003). Transgenic CaMKIIdeltaC overexpression uniquely alters cardiac myocyte Ca^{2+} handling: reduced SR Ca^{2+} load and activated SR Ca^{2+} release. *Circ Res* **92**, 904–911.

Marks AR (2003). A guide for the perplexed. Towards an understanding of the molecular basis of heart failure (Editorial). *Circulation* **107**, 1456–1459.

Marx SO, Gaburjakova J, Gaburjakova M, Henrikson C, Ondrias K & Marks AR (2001). Coupled gating between cardiac calcium release channels (ryanodine receptors). *Circ Res* **88**, 1151–1158.

Marx SO, Reiken S, Hisamatsu Y, Jayaraman T, Burkhof D, Rosemblit N & Marks AR (2000). PKA phosphorylation dissociates FKBP12.6 from the calcium release channel (ryanodine receptor): defective regulation in failing hearts. *Cell* **101**, 365–376.

Prestle J, Janssen PM, Janssen AP, Zeitz O, Lehnart SE, Bruce L, Smith GL & Hasenfuss G (2001). Overexpression of FK506-binding protein FKBP12.6 in cardiomyocytes reduces ryanodine receptor-mediated Ca^{2+} leak from the sarcoplasmic reticulum and increases contractility. *Circ Res* **88**, 188–194.

Rodriguez P, Bhogal MS & Colyer J (2003). Stoichiometric phosphorylation of cardiac ryanodine receptor on serine-2809 by calmodulin-dependent kinase II and protein kinase A. *J Biol Chem* **278**, 38593–38600.

Rose WC, Balke CW, Wier WG & Marban E (1992). Macroscopic and unitary properties of physiological ion flux through L-type Ca^{2+} channels in guinea-pig heart cells. *J Physiol* **456**, 267–284.

Santana LF, Cheng H, Gomez AM, Cannell MB & Lederer WJ (1996). Relation between the sarcolemmal Ca^{2+} current and Ca^{2+} sparks and local control theories for cardiac excitation-contraction coupling. *Circ Res* **78**, 166–171.

Sham JS (2000). Reverse Na^{+}-Ca^{2+} exchange triggers Ca^{2+} release through regurgitation of sarcoplasmic reticulum. *Biophys J* **78**, 374A.

Shannon TR, Ginsburg KS & Bers DM (2000). Potentiation of fractional sarcoplasmic reticulum calcium release by total and free intra-sarcoplasmic reticulum calcium concentration. *Biophys J* **78**, 334–343.

Shannon TR, Guo T & Bers DM (2003). Ca scraps: local depletions of free [Ca] in cardiac sarcoplasmic reticulum during contractions leave substantial Ca reserve. *Circ Res* **93**, 40–45.

Sitsapesan R & Williams AJ (1994). Regulation of the gating of the sheep cardiac sarcoplasmic reticulum Ca^{2+}-release channel by luminal Ca^{2+}. *J Membr Biol* **137**, 215–226.

Song L-S, Wang S-Q, Xiao R-P, Spurgeon H, Lakatta EG & Cheng H (2001). β-Adrenergic stimulation synchronizes intracellular Ca^{2+} release during excitation-contraction coupling in cardiac myocytes. *Circ Res* **88**, 794–801.

Trafford AW, Díaz ME, Negretti N & Eisner DA (1997). Enhanced calcium current and decreased calcium efflux restore sarcoplasmic reticulum Ca content following depletion. *Circ Res* **81**, 477–484.

Tsien RW, Bean BP, Hess P, Lansman JB, Nilius B & Nowycky MC (1986). Mechanisms of calcium channel modulation by beta-adrenergic agents and dihydropyridine calcium agonists. *J Mol Cell Cardiol* **18**, 691–710.

Valdivia HH, Kaplan JH, Ellis-Davies GC & Lederer WJ (1995). Rapid adaptation of cardiac ryanodine receptors: modulation by Mg^{2+} and phosphorylation. *Science* **5206**, 1997–2000.

Varro A, Negretti N & Eisner DA (1993). An estimate of the calcium content of the sarcoplasmic reticulum in rat ventricular myocytes. *Pflugers Arch* **423**, 158–160.

Viatchenko-Karpinski S & Györke S (2001). Modulation of the Ca^{2+}-induced Ca^{2+} release cascade by beta-adrenergic stimulation in rat ventricular myocytes. *J Physiol* **533**, 837–848.

Wier WG, Egan TM, López-López JR & Balke CW (1994). Local control of excitation-contraction coupling in rat heart cells. *J Physiol* **474**, 463–471.

Witcher DR, Kovacs RJ, Schulman H, Cefali DC & Jones LR (1991). Unique phosphorylation site on the cardiac ryanodine receptor regulates calcium channel activity. *J Biol Chem* **266**, 11144–11152.

Yoshida A, Takahashi M, Imagawa T, Shigekawa M, Takisawa H & Nakamura T (1992). Phosphorylation of ryanodine receptors in rat myocytes during beta-adrenergic stimulation. *J Biochem (Tokyo)* **111**, 186–190.

Yuan W-L, Ginsburg KS & Bers DM (1996). Comparison of sarcolemmal calcium channel current in rabbit and rat ventricular myocytes. *J Physiol* **493**, 733–746.

Yue DT, Herzig S & Marban E (1990). Beta-adrenergic stimulation of calcium channels occurs by potentiation of high-activity gating modes. *Proc Natl Acad Sci U S A* **87**, 753–757.

Zhang R, Zhao J, Mandveno A & Potter JD (1995). Cardiac troponin I phosphorylation increases the rate of cardiac muscle relaxation. *Circ Res* **76**, 1028–1035.

Acknowledgements

We thank Dr E. G. Kranias for providing the transgenic mice expressing mutant phospholamban. This work was supported by grants from the NIH: HL-30077 and HL-64098.